# Selective dissolution of brass in salt water

F.M. AL-KHARAFI*, B.G. ATEYA and R.M. ABD ALLAH
*Department of Chemistry, Faculty of Science, Kuwait University, Kuwait*
*(*author for correspondence, e-mail: faiza@kuc01.kuniv.edu.kw)*

## Abstract

The selective dissolution of brass was studied using potentiodynamic polarization, coloumetric analysis and electrochemical impedance spectroscopy (EIS). Using coloumetric analysis, the partial currents $i_{Zn}$ and $i_{Cu}$ were measured under various potentials and chloride concentrations. Chloride ions promote the dissolution of Zn and Cu and hence increase the rate of dissolution of the alloy. At active potentials, zinc dissolves preferentially leaving the alloy surface enriched in copper. Under this condition, the polarization resistance of the interface and its double layer capacity increase with the time and extent of dissolution of the alloy. As the chloride concentration increases and/or the potential shifts in the noble direction, the rate of copper dissolution increases so that simultaneous dissolution of both components is observed. This increase in the rate of copper dissolution is enhanced by the higher stability of the copper chloride complex ($CuCl_2^-$) compared to zinc chloride ($ZnCl_2$).

## 1. Introduction

The selective corrosion of alloys involves preferential dissolution of the active component of the alloy leaving behind a fragile surface which is enriched in the more noble component. The process leads to serious deterioration of the surface and mechanical properties of the remaining alloy and hence increases the risk of corrosion failures, which may be costly or catastrophic. It is of considerable industrial importance in view of the fact that alloys (e.g., brasses, bronzes, cupronickels, steels, super alloys etc.) form the backbone of modern industries. The mechanism of this process is inherently different and more complex than the mechanism of dissolution of a single metal [1–3].

The dezincification of brass is one of the more recognized forms of this phenomenon [4–6]. It has attracted the attention of researches for some decades and is still the subject of increasing attention [7–18]. It is particularly relevant to Kuwait and the Gulf region where various industries extensively use brass in marine applications and in the form of heat exchanger tubes, for example, in desalination and power generation [19]. Many of the above mechanistic studies were performed in noncomplexing media, such as sulfate and hence their conclusions cannot be extended to salt water which is of great significance in connection with the extensive use of brass in marine environments. Furthermore, they involved measurements of total rates of dissolution of the alloy which were not resolved into partial rates of dissolution of the individual components. Since chloride ions form strong complexes with Cu ions and weaker complexes with Zn ions (as shown below), they affect the equilibrium potentials and hence the tendency for dissolution of the Cu and Zn components of the alloy. Consequently, chloride ions are bound to affect the selective dissolution behaviour of the alloy.

The objective of this work is to study the selective dissolution of brass in salt water. Particular emphasis is directed towards evaluation of the effect of the concentration of chloride ions on the partial rates of dissolution of the individual components of the alloy and on its polarization behaviour. Some recent high quality metallography has attributed the failure of Admiralty brass tubes in a turbo generator oil cooler to stress corrosion cracking promoted by chloride ions [20].

## 2. Experimental details

Electrodes were prepared from rods of commercial brass Cu37Zn. The cross sectional area of the rod (0.2 cm$^2$) served as the working electrode. The electrodes were polished successively using SiC paper followed by 0.3 and 0.05 alumina to give a mirror like finish. They were annealed at 873 K (600 °C) for 72 h in evacuated silica capsules to ensure homogenization and relief of mechanical stresses. Measurements were obtained in (1 M

sodium acetate + 0.1 M acetic acid) buffers of pH 6 containing different concentrations of NaCl. This ensures a constant electrolyte pH, particularly at the electrode surface during dissolution of the brass under all conditions. Solutions were prepared using deionized water and AR grade chemicals. They were deaerated by bubbling argon before and during the tests. The concentration of $Zn^{2+}$ and $Cu^{2+}$ ions during the potentiostatic dissolution of the electrode were determined by atomic adsorption spectrometry (AAS). A conventional three-electrode cell was used with an (Ag/AgCl) reference and a coiled platinum wire counter electrode. The counter electrode was in a separate compartment connected to the cell via a fritted glass disc. Unless otherwise indicated, the polarization curves were measured potentiodynamically at a scan rate of 1 mV s$^{-1}$ using an EG&G (model 273A) potentiostat starting from cathodic to anodic potentials. All potentials are reported versus the Ag/AgCl reference electrode ($E = 0.197$ V vs SHE). The electrochemical impedance of the brass–electrolyte interface was measured using an IM5d impedance analyser (Zahner Electrik, GmbH, Kronach, Germany) based on the universal data acquisition and analysis system AMOS–ANDI. Tests were performed at $(23 \pm 1)$ °C.

## 3. Results and discussion

### 3.1. *Polarization curves*

Figure 1 illustrates the polarization curves of the brass electrode in the buffer medium in absence of chloride ions at scanning rates of 1 and 10 mV s$^{-1}$. The anodic branches of the curves show a limiting current which increases with the scanning rate. This limiting current is observed at or below a potential of −200 mV vs Ag/AgCl. At this range of potential and pH, the Pourbaix diagrams predict that Cu is immune [21] while Zn is active [22]. Consequently, this limiting current and the current below it are attributed to the selective dissolution of Zn from the alloy surface while Cu remains
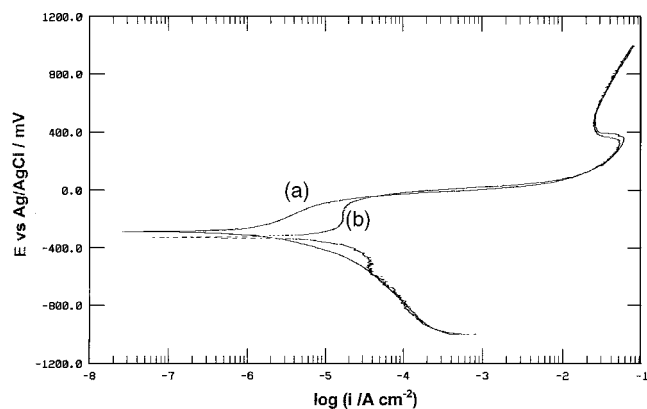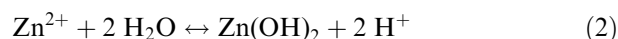


*Fig. 1.* Polarization curves of brass electrode in the buffer medium (in absence of chloride) at scanning rates of (a) 1 and (b) 10 mV s$^{-1}$.

immune. Under these conditions of potential and pH, the Pourbaix diagram indicates that Zn [22] dissolves to give $Zn^{2+}$. That is,

$$Zn \rightarrow Zn^{2+} + 2e^- \qquad (1)$$

The $Zn^{2+}$ ions can exist in equilibrium with $Zn(OH)_2$. That is,

$$Zn^{2+} + 2\,H_2O \leftrightarrow Zn(OH)_2 + 2\,H^+ \qquad (2)$$

Reaction 2 is heavily shifted to the left under the pH 6 of the present measurements.

The dissolution of Zn occurs selectively from the alloy leaving its surface enriched in copper which is immune in this region of potential. Several workers have addressed the mechanism and consequences of this process [1, 2, 12, 14]. It is believed that the zinc atoms dissolve away into the electrolyte leaving vacancies and less coordinated copper atoms on the alloy surface. That is,

$$CuZn \rightarrow Cu^*\square + Zn^{2+} + 2e^- \qquad (3)$$
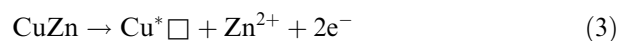
where $\square$ refers to the vacancy and Cu* refers to the remaining more mobile copper atoms in their new less coordinated state. Consequently the alloy surface becomes unstable by virtue of the mole fraction of copper which is now higher than the equilibrium value, the vacancies injected in the lattice and the lower interatomic forces binding these copper atoms into the lattice at the alloy surface.

The fate of these copper atoms has been the subject of some debate. While some authors [1, 12] visualised the formation of new, more copper rich phases, others [14] presented evidence for patches of pure copper accumulating on the surface. As a result of this progressive copper enrichment of the alloy surface, the rate of zinc dissolution decreases with time. Different mechanisms have been proposed for this process. Thus, while some authors [1, 12] visualize a mechanism of upward diffusion of zinc atoms from subsurface layers through the defective copper rich layer, others [13, 14] argue in favour of surface diffusion of the copper atoms on the alloy surface to fill the vacancies and minimize the surface area. The limiting current plateau, shown in Figure 1 at about −200 mV refers to the maximum rate of Zn dissolution from the alloy through the protective Cu rich layer remaining on its surface.

Beyond the limiting currents of Zn dissolution, a rapid increase of current with potential is observed, giving a Tafel region with a slope of about 50 mV extending over about 3–4 decades of current (up to potentials of $E \leqslant 0.15$ V (Ag/AgCl). Within this region, both Zn and Cu are dissolving simultaneously. While Zn dissolves according to Equation 1, the Pourbaix diagrams [21] predict that Cu dissolves according to Reactions 4 and 5 at moderate and high potentials, respectively:
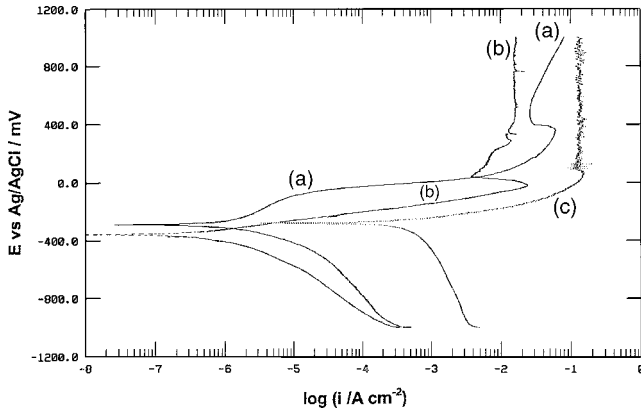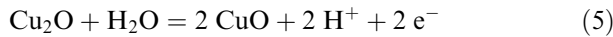
Fig. 2. Effect of chloride concentration on polarization curve of brass electrode in a medium of 1.0 M sodium acetate + 0.1 M acetic acid, pH 6 at a scanning of 1 mV s$^{-1}$. (a) Blank buffer, (b) buffer + 0.58 M NaCl and (c) buffer + 2.0 M NaCl.

$$2\,Cu + H_2O = Cu_2O + 2\,H^+ + 2\,e^- \qquad (4)$$

$$Cu_2O + H_2O = 2\,CuO + 2\,H^+ + 2\,e^- \qquad (5)$$

The behaviour of the alloy in this region is strongly affected by the presence of chloride ions, as shown below. At sufficiently anodic potentials, a current plateau (at several tens of mA cm$^{-2}$) is observed with a fairly modest passivity.

### 3.2. Effect of chloride ions

Figure 2 illustrates the effect of chloride concentration on the polarization curve of the brass electrode in a medium of 1 M acetate + 0.1 M acetic acid of pH 6 at a scanning rate of 1 mV s$^{-1}$. There is a significant promoting effect of pH 6 measured at the anodic dissolution rate, accompanied by disappearance of the limiting current, which was observed in Figure 1 in the absence of chloride ions. A Tafel region is observed in the chloride containing media, with a slope of 62 mV extending for about four decades of current.

For the case of copper, it has been established that Cu dissolves to give CuCl$_2^-$ in strong chloride media [23–29]. That is,

$$Cu + 2\,Cl^- \longrightarrow CuCl_2^- + e^- \qquad (6)$$
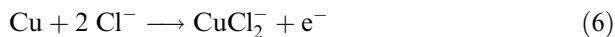
Reaction 6 has been shown to be controlled by diffusion in the electrolyte and is associated with a Tafel slope of 60 mV [23–28], which is in good agreement with the values measured in the present work. On the other hand, the zinc dissolution reaction may be represented by

$$Zn + 2\,Cl^- \longrightarrow ZnCl_2 + 2\,e^- \qquad (7)$$
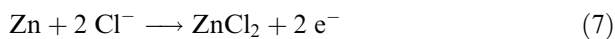
Both copper and zinc ions from complexes with chloride ions, the most stable of which are CuCl$_2^-$ and ZnCl$_2$ [30]. That is,

$$Cu^+ + 2\,Cl^- \leftrightarrow CuCl_2^- \qquad pk = 5.5 \qquad (8)$$

$$Zn^{2+} + 2\,Cl^- \leftrightarrow ZnCl_2 \qquad pk = 0.61 \qquad (9)$$

These values indicate that the predominant copper species is CuCl$_2^-$ while both Zn$^{2+}$ and ZnCl$_2$ are present in the electrolyte at comparable levels.

The equilibrium potential of the copper electrode reaction is given by [16, 31]:

$$E_{(Cu/CuCl_2^-)} = 0.224 - 0.0591 \log \frac{[Cl^-]^2}{[CuCl_2^-]} \qquad (10)$$

Taking [CuCl$_2^-$] $\approx 10^{-4}$ M and [Cl$^-$] = 0.58, gives an equilibrium potential of −0.125 V vs SHE which is equivalent to −0.322 V vs Ag/AgCl. Therefore at potentials more noble than this value, copper is expected to dissolve out of the alloy according to Reaction 6. Under a comparable concentration of Cu$^+$ ions (10$^{-4}$ M) in absence of chloride ions and using a value of 0.52 V vs SHE for the Cu/Cu$^+$ system, gives an equilibrium potential of the Cu electrode of about 0.284 V vs SHE, which is equivalent to 0.087 V vs Ag/AgCl. Therefore the presence of 0.58 M chloride ions shifts the equilibrium potential of the copper dissolution reaction (Cu ↔ Cu$^+$ + e$^-$) from 0.087 to −0.322 V vs Ag/AgCl, by about 400 mV in the active direction. Hence at potentials greater than −0.322 V vs Ag/AgCl copper dissolves in the presence of chloride ions, whereas it was immune at the same potential in the absence of chloride ions. Consequently, chloride ions weaken what was otherwise a protective Cu rich layer on the alloy surface which retarded the selective dissolution of Zn. This explains the increased dissolution current of the alloy in this region of potential in the presence of chloride (Figure 2). It also explains the disappearance of the limiting current plateau (Figures 1 and 2) which was attributed to the retarding effects of the copper rich layer remaining on the alloy surface on the rate of dissolution of Zn. Under conditions where Cu also dissolves away, Zn readily dissolves from the alloy surface in the absence of the strong retarding effect of the copper rich layer on the alloy surface.

Similarly, the equilibrium potential of the zinc electrode reaction is given by

$$E_{(Zn/ZnCl_2)} = E° + \frac{0.059}{2} \log \frac{[ZnCl_2]}{[Cl^-]^2} \qquad (11)$$

Taking a zinc concentration of 10$^{-3}$ M, gives an equilibrium potential of −0.835 V vs SHE, which is equivalent to −1.032 V vs Ag/AgCl.

The above values define the ranges of potential under which either selective dissolution of Zn or simultaneous dissolution of Zn and Cu can occur in the chloride medium. Thus at potentials less noble than −0.332 V and more noble than −1.032 V vs Ag/AgCl, Zn dissolves preferentially to give ZnCl$_2$ while Cu remains immune

and hence is enriched on the alloy surface. At potentials more noble than −0.332 V vs Ag/AgCl, both Zn and Cu dissolve simultaneously out of the alloy surface, albeit at different rates. The rate of dissolution of each component was measured under different conditions of potential and chloride concentration (see below). The difference in the rates of dissolution of the components is caused by differences in the polarization, $\eta = E - E_{rev}$, which is the driving force for dissolution. Thus, in principle, although we have simultaneous dissolution of both components in the region of potential above −0.332 V vs Ag/AgCl, the rates of dissolution of both components may or may not be proportional to their mole fraction in the alloy. If they are proportional, the composition of the dissolving alloy surface would be identical to that of the parent alloy. Otherwise preferential selective dissolution of one component takes place at a rate which is greater than that required by its mole fraction at the alloy surface.

### 3.3. Electrochemical impedance

The electrochemical impedance spectra of brass electrodes polarized at a potential of −260 mV vs Ag/AgCl were measured at various times of immersion in a medium of pH 6 containing 0.58 M NaCl were measured. This potential is at the beginning of the region where Cu starts to dissolve (see above) and hence simultaneous dissolution of both components is expected with Zn dissolving preferentially at a higher rate. Measurements of the partial currents of dissolution of Zn and of Cu shows that this is the case. The ratio of mole fractions of Cu:Zn in the alloy is Cu/Zn ≈ 1.75. Simultaneous dissolution without preferential enrichment of the alloy surface prevails when the ratio of partial currents $i_{Cu}/i_{Zn} \approx 1.75$. Higher and lower values of this ratio require preferential dissolution of Cu or of Zn, respectively. At this potential, $i_{Cu}$ and $i_{Zn}$ were found to be $3.82 \times 10^{-3}$ and $1.1 \times 10^{-2}$ mA cm$^{-2}$, respectively, corresponding to a ratio of $i_{Cu}/i_{Zn} \approx 0.35$ which reveals preferential dissolution of Zn.

Figures 3 and 4 represent the Bode and Nyquist plots obtained at various times of dissolution. These results can be analysed in light of the equivalent circuit shown in the inset of Figure 1 [31]. Table 1 summarizes the results. The polarization resistance ($R_p$) and the double layer capacity ($C$) of the interface increase gradually with time. An increase in the double layer capacity of the interface under conditions of dealloying has long been taken as an indication of increased surface area [32]. On the other hand, the increase in the polarization resistance of the interface with time reflects an increased difficulty of dissolution. These results are compatible with gradual increase of the surface area with simultaneous enrichment of the surface in Cu. Recent measurements on dissolving brass using in situ STM imaging revealed increasing surface roughening with time of dissolution [14].
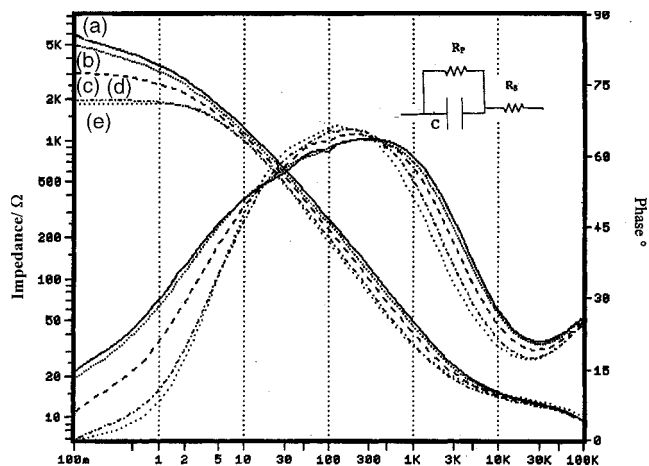


Fig. 3. Time variation of Bode plot of brass electrode polarized at −260 mV vs Ag/AgCl in a medium of pH 6 in presence of 0.58 M NaCl. (a) 1, (b) 15, (c) 30, (d) 45, and (e) 60 min.
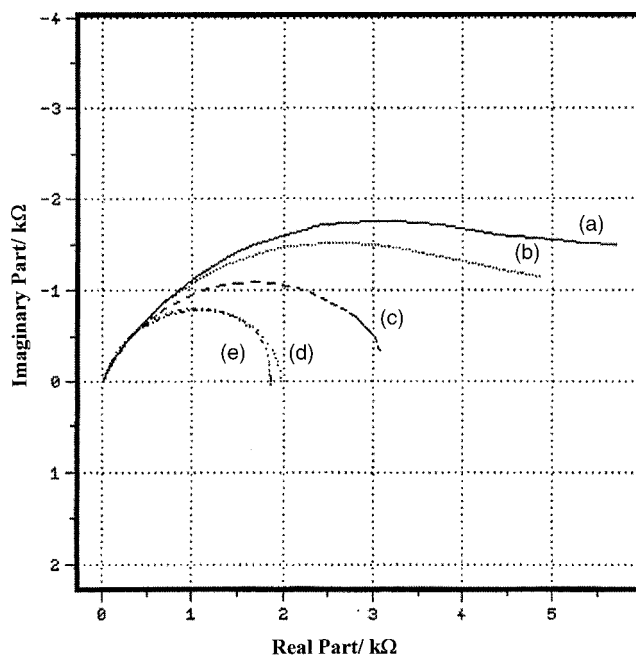


Fig. 4. Time variation of Nyquist plot of brass electrode polarized at −260 mV vs Ag/AgCl in a medium of pH 6 in presence of 0.58 M NaCl. (a) 1, (b) 15, (c) 30, (d) 45 and (e) 60 min.

Table 1. Time variation of the polarization resistance ($R_p$) and double layer capacity ($C$) of the brass electrode in an acetate buffer of pH 6 + 0.58 M NaCl at a potential of −260 mV vs Ag/AgCl at 25 °C

| Time/min | $R_p/k\Omega$ cm$^{-2}$ | $C/\mu F$ cm$^{-2}$ |
|---|---|---|
| 0 | 3.29 | 12.8 |
| 30 | 5.41 | 14.0 |
| 60 | 6.21 | 16.2 |
| 90 | 6.23 | 17.2 |
| 120 | 6.51 | 17.1 |
| 150 | 6.72 | 19.9 |
| 180 | 6.82 | 20.3 |

### 3.4. *Partial currents*

Several values of potential were selected for potentiostatic polarization measurements extending for 1 h during which the concentrations of both zinc and copper ions in the electrolyte were determined as a function of time. These measurements were performed in a buffered solution of 3.4% (0.58 M) NaCl, which contains about the same salt level as that in sea water. The concentration of each ion was converted into charges associated with the passage of these ions using Faraday's law. That is,

$$Q = \int_0^t i\,\mathrm{d}t = nF\Delta m/M \tag{12}$$

where $n$ is the charge on the ion resulting from the anodic dissolution of the particular metal (2 for Zn and 1 for Cu), $F$ is the Faraday constant, $96\,500$ C mol$^{-1}$, $\Delta m$ is the mass of the particular component of the alloy that passed into solution after a particular time, $t$, and $M$ is its atomic weight. Figure 5(a–d) illustrates the variation of $Q$ with time for both zinc and copper upon polarization of the brass under gradually decreasing potentials, that is, 60, 0, −80, and −130 mV vs Ag/AgCl, respectively. The relations of both components are straight lines during the entire duration of the tests. Equation 12 enables calculation of the partial current of a certain component, $i(x)$ at any time by taking the

tangent of the curve of $Q$ against $t$ at the particular time. That is,

$$i(x) = \partial Q(x)/\partial t \tag{13}$$

The slope of each line gives the partial current of the particular component. Since both relations are straight lines, and in view of Equation 13, it can be concluded that the partial currents, $i(Zn)$ and $i(Cu)$ are constant throughout the duration of the test. Some dozens of these curves were constructed from measurements under various conditions. Table 2 lists the values of $i_{(Zn)}$ and $i_{(Cu)}$ obtained under various potentials. At active potentials, $i_{(Cu)}$ is much lower than $i_{(Zn)}$. This is readily explained in the light of the much larger driving force

*Table 2.* Partial currents of dissolution of Zn and of Cu, $i_{(Zn)}$ and $i_{(Cu)}$, from brass under various potentials in an electrolyte of pH 6 containing 0.58 M (3.4%) NaCl

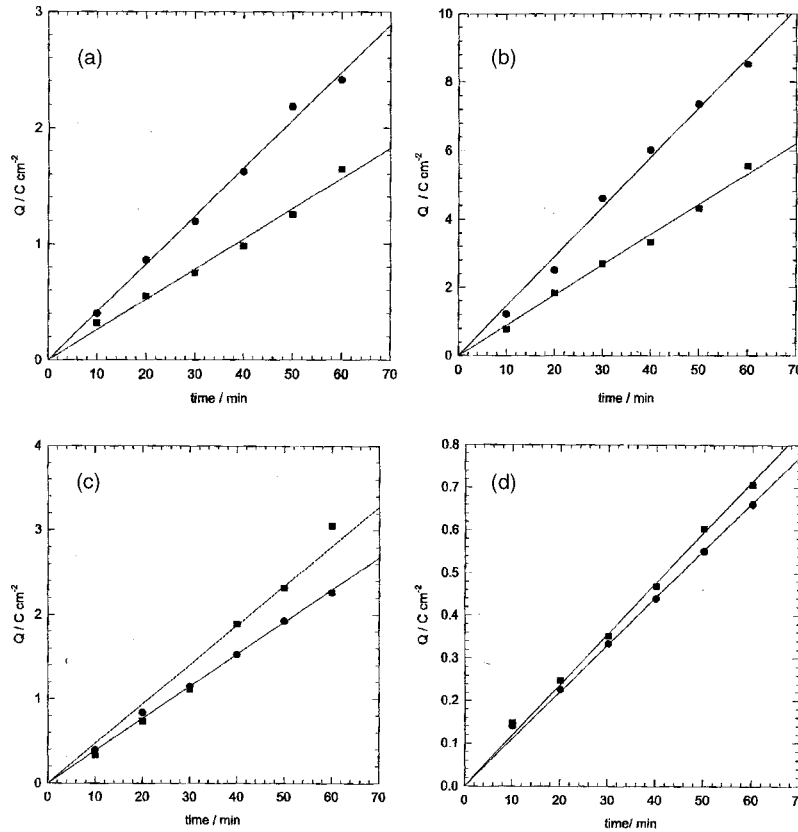| $E$/mV | $i_{(Zn)}$/mA cm$^{-2}$ | $i_{(Cu)}$/mA cm$^{-2}$ |
|---|---|---|
| −300 | $1.19 \times 10^{-3}$ | 0.0 |
| −260 | 0.011 | $3.82 \times 10^{-3}$ |
| −230 | 0.017 | $5.50 \times 10^{-3}$ |
| −180 | 0.046 | 0.0245 |
| −130 | 0.188 | 0.175 |
| −80 | 0.912 | 0.620 |
| −40 | 1.70 | 2.71 |
| 0.0 | 1.52 | 2.47 |
| 60 | 0.425 | 0.688 |



*Fig. 5.* Time variation of charge passed by dissolution of Zn and of Cu from brass alloy polarized at (a) 60 , (b) 0 , (c) −80, and (d) −130 mV vs Ag/AgCl, respectively. All measurements performed in a buffered medium of pH 6 containing 0.58 M NaCl. Key: (●) Cu and (■) Zn.

for the dissolution of Zn than that of Cu, in view of the much more active value of equilibrium potential of the Zn dissolution reaction (−1.032 V vs Ag/AgCl), as compared to that of Cu (−0.332 V vs Ag/AgCl). At these active potentials, a low rate of copper dissolution is expected in view of the fact that the driving force for dissolution of Cu is fairly low. As the potential becomes more anodic (e.g., −180 mV vs Ag/AgCl), the Cu dissolution reaction experiences a stronger driving force. Consequently, its rate approaches, and ultimately exceeds, that of Zn dissolution. The decrease of both $i_{Zn}$ and $i_{Cu}$ above 0 V vs Ag/AgCl can be attributed to the onset of mild passivity as observed in the polarization curves, (Figure 2).

The effects of chloride concentration on the partial currents, $i_{(Zn)}$ and $i_{(Cu)}$ were measured at a potential of 60 mV vs Ag/AgCl. Figure 6 illustrates the results . The relations give straight lines with slopes of 0.85 and 0.62 for the Zn and Cu components, respectively. The slope of such a straight line is the order of the partial reaction with respect to the chloride ions. A positive order indicates that the chloride ions promote the particular reaction to an extent that depends on this order. The results show that chloride ions promote the partial reactions of both components. They also point to a mildly stronger promoting effect of chloride ions on Cu than on Zn dissolution.

## 4. Conclusion

A limiting current has been observed for the selective dissolution of Zn from brass under fairly active potentials ($\leqslant$−200 mV vs Ag/AgCl) in an acetate buffer, pH 6, in absence of chloride ions. This is attributed to the selective dissolution of Zn from the alloy surface while Cu remains immune. The presence of chloride ions affects the thermodynamics and kinetics of dissolution of Cu and Zn from brass. The high stability of the $CuCl_2^-$ complex shifts the equilibrium potential of Cu dissolution by about 400 mV in the active direction, enhancing its rate of dissolution. Below a potential of about −300 mV vs Ag/AgCl in 3.4% NaCl, only selective dissolution of Zn was observed with no detectable level of copper dissolution. At more noble potentials ($\geqslant$−260 mV vs Ag/AgCl), dissolution of both components was observed at rates which increased as the potential becomes more noble. It is also shown that chloride ions promote the dissolution of both Zn and Cu from the alloy by virtue of the positive reaction orders measured for both. At a potential of 60 mV vs Ag/AgCl, the reaction orders were 0.62 and 0.85, respectively.

Fig. 6. Effect of chloride concentration on partial currents, i(Zn) and i(Cu) of brass at a potential of 60 mV vs Ag/AgCl in pH 6 acetate buffer.

## References

1. W. Pickering, *Corros. Sci.* **23** (1983) 1107.
2. H. Kaiser, *in* F. Mansfield (Ed), 'Alloy Dissolution in Corrosion Mechanisms' (Marcel Dekker, New York, 1987), p. 85.
3. C. van Orden, *in* R. Baboian (Ed), 'Corrosion Tests and Standards: Application and Interpretation' (ASTM 28-020095-27 (ASTM, Philadelphia, PA, 1995).
4. M.G. Fontana, 'Corrosion Engineering' (McGraw-Hill, New York, 3rd edn, 1986), p.86.
5. D.A. Jones, 'Principles and Prevention of Corrosion' (Prentice-Hall, Englewood Cliffs, NJ 2nd edn, 1996), p. 20.
6. N.W. Polan, *in* 'Metals Handbook, Corrosion, Vol. 13' (ASM International, Materials Park, OH, 9th edn, 1987).
7. Z. Liu, L. Lin, J. Xu and Y. Zhao, *Chin. J. Mater. Res.* (China) **14** (2000) 145.
8. L. Burzynska, *Corros. Sci.* **43** (2001) 1053.
9. A.A. Elwarraky, *J. Mater. Sci.* **31** (1196) 119.
10. R.K. Diannappa and S.M. Mayanna, *Corros. Sci.* **27** (1987) 349.
11. I. Singh, 'Anti-Corrosion', (March 1988), p. 4.
12. H.W. Pickering and P.J. Byrne, *J. Electrochem. Soc.* **116** (1969) 1492; **118** (1971) 209.
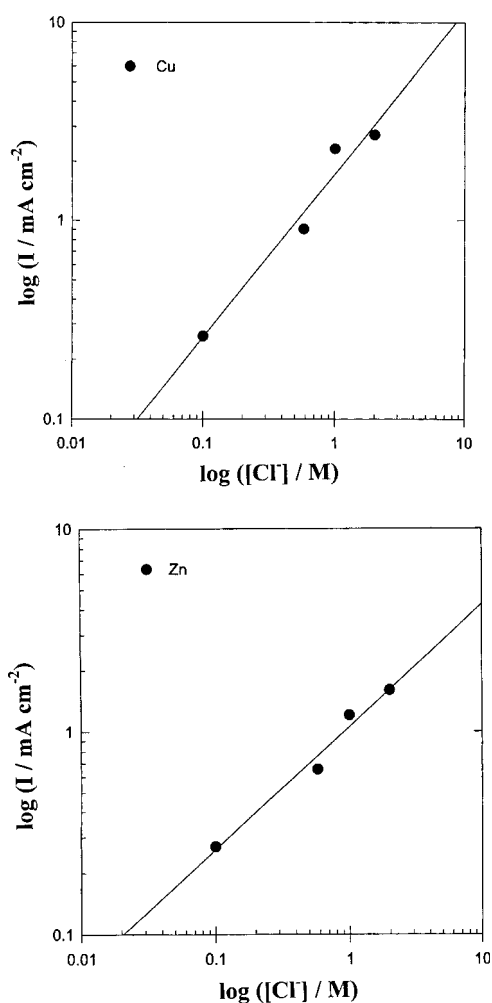13. G.T. Burstein and G. Gao, *J. Electrochem. Soc.* 141 (1994) 912.

14. H. Martin, P. Carro, A. Hernandez Creus, J. Fernandez, P. Esparza, S. Gonzalez, R.C. Salvarezza and A.J. Arvia, *J. Phys. Chem.* **104B** (2000) 8229.

15. C.E. Price, *Mater. Perform.* **34** (1995) 87.

16. A.M. Fenelon and C.B.B. Breslin, *J. Appl. Electrochem.* **31** (2001) 509.

17. K. Balakrishnan and V.K. Venkatesan, *Werkst. Korros.* **29** (1978) 113.

18. V.N. Chervyakov, A.P. Pchel'nikov and V.V. Losev, *Elektrokhimiya* (Russia) **27** (1991) 1647.

19. H.M. Shalaby, A. Al-Hashem, M. Lowther and J. Al-Besharah (Eds), 'Industrial Corrosion and Corrosion Control Technology' (Kuwait Institute for Scientific Research, Kuwait, 1996).

20. Samuel J. Lawrence and Richard L. Bodnar, *Adv. Mater. Proces.* (Feb. 1997) 29.

21. N. De Zoubov, C. Vanleugenhaghe and M. Pourbaix, *in* M. Pourbaix (Ed), 'Atlas of Electrochemical Equilibria in Aqueous Media' (NACE, Houston, 1974), p. 384.

22. N. DeZoulov and M. Pourbaix, *in* [21], p. 406.

23. M.E. Walton and P.A. Brook, *Corros. Sci.* **17** (1977) 593.

24. L.H. Jenkins, *J. Electrochem. Soc.* **117** (1970) 630.

25. A.L. Bacarella and J.C. Griess, *J. Electrochem. Soc.* **120** (1973) 459.

26. J.O'M. Bockris, B.T. Rubin, A. Despic and B. Lovrecek, *Electrochim. Acta* **17** (1972) 973.

27. C. Kato, B.G. Ateya, J.E. Castle and H.W. Pickering, *J. Electrochem. Soc.* **127** (1980) 1881.

28. C.H. Bonfiglio, A.C. Albaya and A.O. Cobo, *Corros. Sci.* **13** (1973) 717.

29. D. Tromans and G. Li, *Electrochem. Sol. St. Lett.* **5** (2002) B5.

30. J.A. Dean, (Ed), 'Lange's Handbook of Chemistry' (McGraw-Hill, New York, 14th edn, 1992), p. 8.83.

31. F.M. Al-Kharafi and B.G. Ateya, *J. Electrochem. Soc.* **149** (2002) B206.

32. H.W. Pickering, *J. Electrochem. Soc.* **115** (1968) 690.